FACTA UNIVERSITATIS
Series:**Mechanical Engineering** Vol. 20, Nº 2, 2022, pp. 279 - 306
https://doi.org/10.22190/FUME220201009S

Original scientific paper

EFFECT OF STATIC AND HARMONIC LOADING ON THE HONEYCOMB SANDWICH BEAM BY USING FINITE ELEMENT METHOD

Babak Safaei[1,2], Emmanuel Chukwueloka Onyibo[1], Dogus Hurdoganoglu[1]

[1]Department of Mechanical Engineering, Eastern Mediterranean University, Famagusta, Turkey
[2]Department of Mechanical Engineering Science, University of Johannesburg, Gauteng, South Africa

Abstract. *The aim of this paper is to present a proposed honeycomb core shape and compare it with a normal hexagonal shape core in a sandwich beam. The sandwich cores are simulated in finite element with different materials; aluminum and epoxy-carbon with six layers are used as face sheet and the results are compared to those obtained theoretically. Simulation of 3-point bending test is performed in commercial software ANSYS to verify the analytical results with the numerical ones. Hence, for simplicity one layer of the skin is used on the equivalent model of sandwich for lesser computational time and more accurate evaluation. Simulation of harmonic analysis of hexagonal core and proposed core shape is carried out in frequency domain to identify the core with less deformation under high frequency and it can withstand harmful effects. The proposed core shape model having the same cell numbers and material as the normal hexagonal model is compared with experimental results; it is observed that the proposed core shape model has good flexural stiffness, resonance, fatigue, and stress resistance at a higher frequency.*

Key Words: *Honeycomb Sandwich, Static Analysis, Harmonic Analysis, Finite Element Method*

Received: February 01, 2022 / Accepted March 09, 2022
Corresponding author: Babak Safaei
Department of Mechanical Engineering, Eastern Mediterranean University, Famagusta, North Cyprus via Mersin 10, Turkey
Department of Mechanical Engineering Science, University of Johannesburg, Gauteng 2006, South Africa
E-mail: babak.safaei@emu.edu.tr

1. INTRODUCTION

The honeycomb structure is a natural or man-made structure that has a honeycomb geometry to reduce the volume of material to attain minimum weight and minimal cost [1]. The geometry of the honeycomb structures can vary greatly, but the typical characteristic of such structures is the sequence of hollow cells created between the thin vertical walls. The honeycomb structures are widely used in almost every part of the manufacturing sector, because of their advantages, including extremely low weight/force ratios, which leads to lower weight, lower fuel usage. Composite sandwich panels are used in aerospace and civil infrastructure applications because they have a higher flexural/transverse shear stiffness and, as a result, a higher corrosion resistance [2]. The cell arrangement is mostly hexagonal in section. Researchers have experimented with a lot of shapes on sandwich structures, circular [3], triangular [4], square or rhombic [5], and pyramid lattice structures [6]. Honeycomb normally has a regular hexagonal geometry (the sides are equal, the angles are all 120º and the cell walls are of the same thickness). Due to this, their deformations can be easily analyzed and equations of orthotropic properties are obtained [7]. Sandwich panel behaviors depend mainly on the geometric arrangement of core and facing materials [8]. Honeycomb sandwich panels normally consist of two thin face sheets or skins and a lightweight thicker core. Moreover, the core is made of different materials which depend on the desired mechanical properties needed. In some cases, sheet metal is often used as a skin material. The core is bound to the skin by brazing along with the glue or metal elements. Burlayenko and Sadowski [9] filled the honeycomb cores with foam to enhance the damage resistance and equally change the structural response of the sandwich structure, which is preferably used in waterproof, sound, and heat insulation. In addition, the sandwich core is known for low density, high compression, stiffness, and shear properties.

Manufacturing of honeycomb sandwich is mainly by corrugation, expansion, molding and 3D printing while the most adopted manufacturing method is expansion and corrugation [10,11]. Skin materials are laminates of glass or carbon fiber reinforced thermoplastics or mainly thermoset polymers (unsaturated polyesters, epoxies), while commonly used composite is fiber-glass, carbon fiber reinforced plastic, and aluminum [12]. Alhijazi et al. [13] presented and analyzed the elastic properties of luffa and palm natural fiber composites (NFC) with epoxy and ecoepoxy matrixes, with the influence of fiber volume fractions taken into account. However, honeycombs are known to have four common types, aluminum honeycomb, thermoplastic honeycomb, nomex honeycomb and stainless steel honeycomb; moreover, aluminum possesses the highest strength to ratio[14]. Zaid et al. [15] concluded that the corrugated core sandwich structure has a better strength to weight ratio. The experimental eigenvalue responses of the epoxy-filled skew sandwich construction are computed for the first time by Katariya et al. [16] to demonstrate the appropriateness of equivalent type single-layer higher-order theory for the analysis (including through-thickness stretching term effect). The strength increases exponentially relative to the core thickness while the increase in weight is negligible, and honeycomb is easily milled, routed, cut, edged, fastened and bonded, making it the first choice to reinforce any component structural area.

Mechanical property and energy absorption capability of aluminum honeycomb structures vary with impact velocity [17]. Liu et al. [18] investigated the flexural characteristics of a stiffened foam core sandwich structure. However, the honeycomb core is known for its great stiffness. Li et al. [19] stated that sandwich composites with truss

core materials have the best flexural stiffness and strength in bending deformation, which is ideal in structural parts. Wang et al. [20] proposed a novel multilevel modeling approach for calculating Young's modulus of polymers reinforced with graphene nano-platelets. Chemami et al. [21] added orthogrid to improve the stiffness of soft honeycomb and thereby reduce the interfacial mismatch in the sandwich structure. Barbaros et al. [22] analyzed how functionally graded materials (FGMs) are prepared, manufactured, used, as well as their elastic properties. Li et al. [23] studied the behavior of composite sandwich beams with glass fiber reinforced polymer (GFRP) face sheets and a balsa wood core in terms of flexural creep. Ghanati and Safaei [24] investigated the elastic buckling of regular hexagonal thin sheets made of homogeneous and isotropic materials under in-plane hydrostatic and uniaxial compression, with internal supports, translational and rotational elastic edge supports, and a mix of free, simple-support, and clamped boundary conditions. Ribeiro Faria et al. [25] investigated the dynamic behavior of sandwich beams with honeycomb cores loaded with magnetorheological gels and composite material skins under the effect of vibrations. Hence, under various forms of mechanical loads, the static deflection, frequency, and transient responses of the multilayer sandwich shell (flat/curved) structure were estimated by Katariya and Panda [26]. Fazilati et al. [27] showed that honeycomb structures are commonly used as energy shock absorbers due to their strong crashworthiness characteristics of high energy absorption potential and high strength-to-weight ratio. Ha et al. [28] presented the nap-core sandwich's fabrication, characteristics, and uses, with a focus on the sandwich's sensitivity and a special focus on the effect of symmetry in nap cores [29]. Lu et al. [30] compared Nomex and aluminum with sandwiches made from carbon fiber/epoxy and concluded that the bending strength of carbon fiber/epoxy honeycomb is greater. Choosing the best honeycomb core for your application can be a very major factor. Hence, not only mechanical property strengths and stiffness, but also the problem of the environment must also be considered. In order to study and observe the low velocity impact energy response of sandwich structures used for railways, Sakly et al. [31] introduced finite element method (FEM), to simulate ballast impacts, a high-speed and low weight test bench was designed. The graded sandwich shell structure's thermal eigenvalue responses are numerically assessed under varied thermal loadings while considering temperature-dependent characteristics as investigated by Sahoo et al. [32]. He et al. [33] carried out experimentally and numerically the low velocity effect of carbon fiber face sheets and aluminum alloy cores. However, many researchers used carbon fiber as skin [34]. It comes in two weaves, unidirectional (all fibers are parallel) and bidirectional (fibers cross at a 90-degree angle). Furthermore, recently many researchers carried out experiments on 3D printed cores [19,35–37].

Moreover, studying the nonlinear behavior of the sandwich is necessary to truly understand the system's reaction. On an elastic substrate, the nonlinear forced vibrations of FGM sandwich cylindrical shells with porosities are investigated by Liu et al. [38]. Li et al. [39] studied nonlinear vibrations of fiber-reinforced composite cylindrical shells (FRCCSs) with bolted joint boundary conditions, both theoretically and empirically, where the nonlinear amplitude-dependent material properties of fiber-reinforced composites (FRCs) and partial bolt loosening boundary conditions are considered. A coupled nonlinear modeling for composite cylindrical shells is constructed using the modified donnell nonlinear shell theory and Maxwell static electricity/magnetism equations to analyze nonlinear forced vibrations in multi-physics domains as investigated by Liu et al. [40]. Liu et al. [41] created a new method for solving nonlinear forced vibrations of functionally

graded (FG) piezoelectric shells in multi-physics fields. Yang et al. [42] analyzed the geometrically nonlinear harmonically soft stimulated oscillation of size-dependent composite truncated conical microshells (CTCMs) formed of FGMs combined with magnetostrictive layers. According to Yang et al. [43] the proposed research examines the geometrical nonlinear flexural response of arbitrary-shaped microplates with variable thickness composed of FG composites at small scales. The microstructural-dependent nonlinear stability behavior of micropanels under axial compression was studied by Sahmani and Safaei [44] combining moving Kriging meshfree formulations with the third-order shear flexible shell model and modified strain gradient continuum mechanics. Liu et al. [45] investigated a size-dependent numerical solution approach to assess nonlinear buckling and post-buckling of cylindrical microsized shells constructed of checkerboard randomly reinforced nanocomposites subjected to axial and lateral compressions. Hence, a smart multifunctional sandwich plate with one core lightweight porous layer, two intermediate polymer/graphene nanocomposite layers, and two active faces constructed of piezoceramic material is presented by Moradi-Dastjerdi and Behdinan [46]. In addition, they used an innovative and trustworthy method, to examine the free vibration behaviors of a multifunctional smart sandwich plate [47]. The mechanically excited layered skew sandwich shell panels' time-dependent deflection responses are estimated by Katariya et al. [48] numerically using a general model built theoretically utilizing higher-order shear deformation theory, which includes the effects of large displacement. The frequency responses of a free vibrated composite sandwich panel structure are numerically studied by Katariya et al. [49] by taking geometrical nonlinearity into account by using generalized Green–Lagrange strain kinematics.

However, the mathematical models of static and fatigue response of honeycomb structures panel were developed by several researchers, due to the multiple numbers of coefficients and parameters based on their experiments, it is difficult to implement. Due to this, ANSYS and ABAQUS were introduced by a few researchers to study the response and investigate the behavior of sandwich structures. Upreti et al. [50] investigated the normal frequency of a honeycomb sandwich composite structure consisting of unidirectional carbon/glass fibers. The dynamic stiffness matrix approach is used to calculate the natural frequencies for out-of-plane free vibration of three-layer symmetric sandwich beams by Gholami et al. [51]. Jin et al. [52] studied a low-frequency vibrating lightweight cylindrical honeycomb sandwich structure. Safaei [53] examines the damped vibrational behavior of a light sandwich plate subjected to a periodic force over a short period of time. Kim and Hwang [54] investigated the natural frequencies of honeycomb sandwich beams with embedded debonding or delamination between the face-layer laminates and the honeycomb core. Abbadi et al. [55] stated that the presence of defects has no effect on the static behavior of the material. Herranen et al. [56] investigated the strength of GFRP sandwich panels with different core materials through experimentation and simulation using the ANSYS APDL program. ANSYS is one of the favorite among designers, Alhijazi et al. [57] found out that the ANSYS workbench is highly programmed and incredibly versatile, enabling users to customize it to their particular application or analysis. Fatigue experiments were carried out to investigate the behavior of honeycombs with and without an artificial defect, therefore concluding that the drilling type defect influenced the fatigue life significantly compared to Brinell. The fatigue life in W-direction is lesser than the L configuration. Sandwich panels with defects (Brinell and drilling hole) have a lower face cracking failure mode for both configurations. Herranen et al. [58] studied finite element

analysis (FEA) subjected to 4-point bending was conducted with ANSYS APDL v12.1 software for glass fiber plastic (GFRP) to investigate the strength. Selvaraj et al. [59] used the ANSYS program to model the laminated composite single-core and double-core sandwich beams numerically; hence, the study findings explicitly demonstrated that their stiffness is higher than that of single-core composite sandwich beams, due to the greater stiffness provided by double-core composite sandwich beams. Safaei et al. [60] developed a Galerkin-based FEM model to analyze the elastic stress field in a platelet reinforced composite subjected to axial load.

This paper aims to investigate the static loading effect on the sandwich beam. Its flexural stresses were clearly analyzed and harmonic analysis of the two core shapes was investigated; the amplitude of the response, phase angle and corresponding stresses were detailed. Epoxy carbon UD (230GPa) was used as face skin, aluminum, honeycomb and SAN foam materials used as core. In addition to that, the aluminum alloy was later used as face skin while maintaining honeycomb as the core for validation. The ANSYS FEM simulation results were validated analytically and it is in accordance with the stiffness of the sandwich beams equation. The natural frequency of honeycomb core and of mode shapes is illustrated. In order to gain a better insight into certain systems' deformation mechanisms, ANSYS is used as the finite element simulation and comparisons between both honeycomb cores materials deformation, stress resistance and mode shapes. Lastly, improved flexural stiffness, resonance resistance and optimization check between the normal hexagonal honeycomb core and proposed shape core are confirmed.

2. PROBLEM MODELING

2.1. Problem objective

The response of honeycomb structures under static loading with different cores, aluminum, honeycomb, and SAN foam with the same face sheet will be investigated in this study, in view of modal analysis and static structure. In order to find the most influenced output like equivalent stress, stiffness and natural frequency, the design of the experiment and parameter correlation is used in the ANSYS tool for understanding the parametric response. Lastly, harmonic analysis of two different shaped geometry cores are investigated and stresses reviewed at their peak frequencies.

2.2. Geometry and material properties

The honeycomb core model is created using commercial Solidworks software (IGS file format) Fig. 1(a) and imported to the ANSYS workbench for assembling in static structural. ANSYS Composite PrepPost (ACP) is used for the design of the face sheet, combining laminate layup from a composite material as shown in Fig. 1(b). In addition, the honeycomb core is bounded on both sides by two face sheet (epoxy carbon 230 UD) as depicted in Fig. 1(c). Lastly, Fig. 1(d) depicts the proposed honeycomb model design.

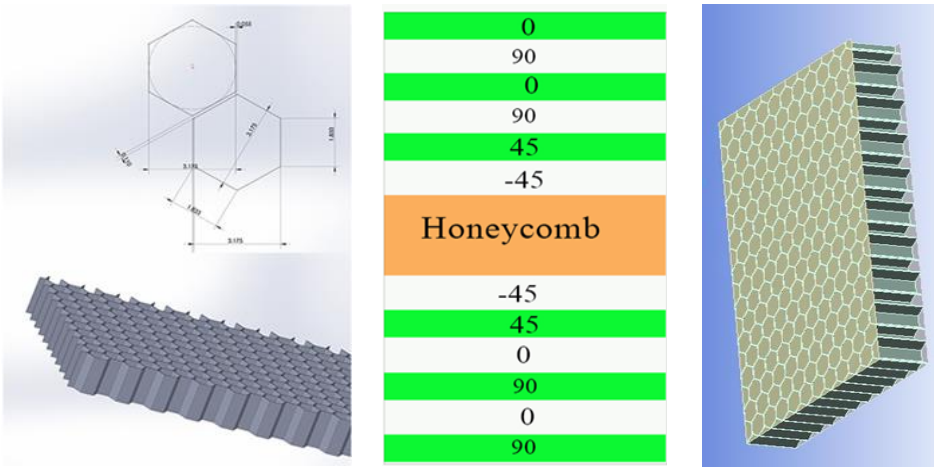

(a) (b) (c)

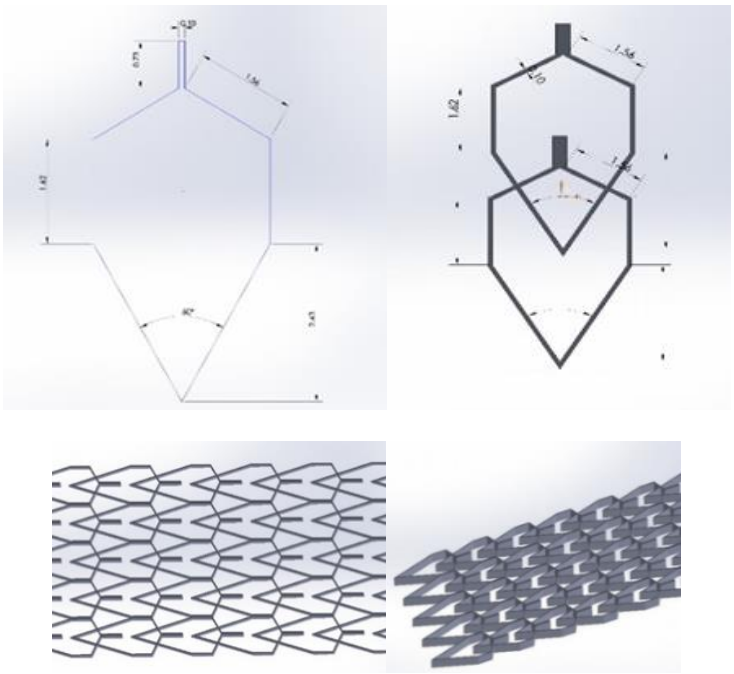

(d)

Fig. 1 Schematic of honeycomb sandwich structure; (a) Hexagonal honeycomb; (b) Laminate layup composite; (c) Bounded surface of honeycomb core and face sheet; (d) Proposed core honeycomb inclined edge model

2.3. Material properties

Epoxy provides a solid, durable framework with good carbon fiber adhesion. Pre-preg is a polymer consisting of "pre-impregnated" fibers. Unidirectional (UD) carbon fiber has high bending power in a 0-degree orientation associated with the fibers against the progression of forces. The same configuration of the core is used for an isotropic solid sandwich made of epoxy carbon (thickness = 0.2 x 5mm). The lay ups used for orthotropic face sheets are [0/0/0/0/0]; therefore, the laminate thickness is 1mm on each skin. Table 1 lists the material properties that were used in the sandwich beam structure analysis. Aluminum, honeycomb, and SAN foam are used as the core in bending stress analysis, epoxy carbon UD (230 GPa) PrePreg is used for the face sheet. Lastly aluminum alloy and honeycomb are used as skin and core, respectively, for analytical validation.

Table 1 Material properties used for skin and core

Material	Young's Modulus E (MPa)	Poisson's Ratio v	Shear Modulus G (MPa)	Density ρ (kg/m^3)
SAN Foam	85	0.3	32.692	103
Aluminum	7100	0.33	2669	2770
Epoxy Carbon	121000	0.27	4700	1490
Honeycomb	1	0.49	1E-06	80
Resin Epoxy	3780	0.35	1400	1160

2.4. Meshing of FEA

Meshing is a method of transforming geometrical bodies into finite element entities. In this design of the sandwich structure, 8 nodded brick elements are used. In order to divide the domain into discrete elements, and to solve the equilibrium equation for each nodal location, the SOLID168 element type was used; this is a high order element that gives sufficient bending properties for this work. SOLID168 is an explicit dynamical element in a higher order, 3-D 10-node. It is ideal to model irregular meshes, for example those created from different CAD/CAM systems. The element is defined with a total of 10 nodes, each with three degrees of freedom: node x, y and z. Finite meshing is performed to take account of the transition of tension between the core material and the face sheet, as seen in Fig. 2(a). Pham used different types of meshing methods and sizing [61]. Moreover, meshing can affect the output results in order to be close to the analytical solution; fine meshing is adopted for the face sheet and program-controlled mesh for the honeycomb core in Fig. 2(b). The number of nodes and elements used for both face skin and honeycomb core are shown in Table 2. Fig. 2(c) shows the meshing of a Solid model of Sandwich beam (all components and materials of the sandwich assigned by ACP module in ANSYS). Furthermore, Figs. 2(d) and 2(e) show the meshing of the hexagonal core and proposed core model. However, the higher the nodes and elements, the longer computational time, but better the results, when compared to the exact solution.

Table 2 Number of nodes and elements

Name	Material	Nodes	Elements	Thickness (mm)
Face-sheet	Epoxy Carbon	868	803	1
Hexagonal honeycomb core	Aluminum alloy	42469	5680	10
Proposed core	Aluminum alloy	45787	6750	10

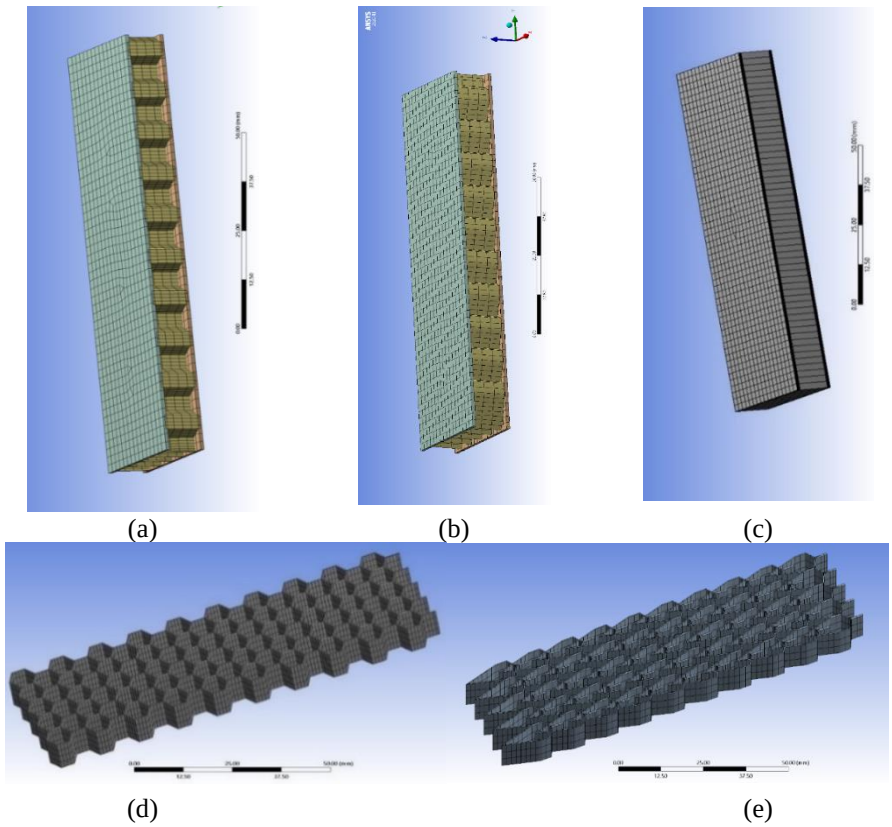

Fig. 2 Finite element meshing: (a) Meshing of sandwich structure (hexagonal honeycomb core); (b) Meshing of sandwich structure (proposed honeycomb core); (c) Solid model meshing; (d) Meshing of honeycomb core; (e) Meshing of proposed honeycomb core

2.5. Boundary conditions and Loads

The honeycomb sandwich structure has been assigned a fixed support at one end and displacement at the other end in a line of Z-axis (horizontal to the sandwich); hence in order to mimic simply supported beam conditions, the top face skin is loaded with uniformly force in the static structural analysis of ANSYS workbench as shown in Fig. 3(a). Figs. 3(c) and (d) analysis are carried out to investigate the modal frequencies and harmonic

response, therefore treating the honeycomb core as a cantilever beam (one end fixed). Lastly, as shown in Fig. 3(e), concentrated loading of 3-point bending test of equivalent shell model of the sandwich structure is performed to validate the analytical calculation with the simulation method.

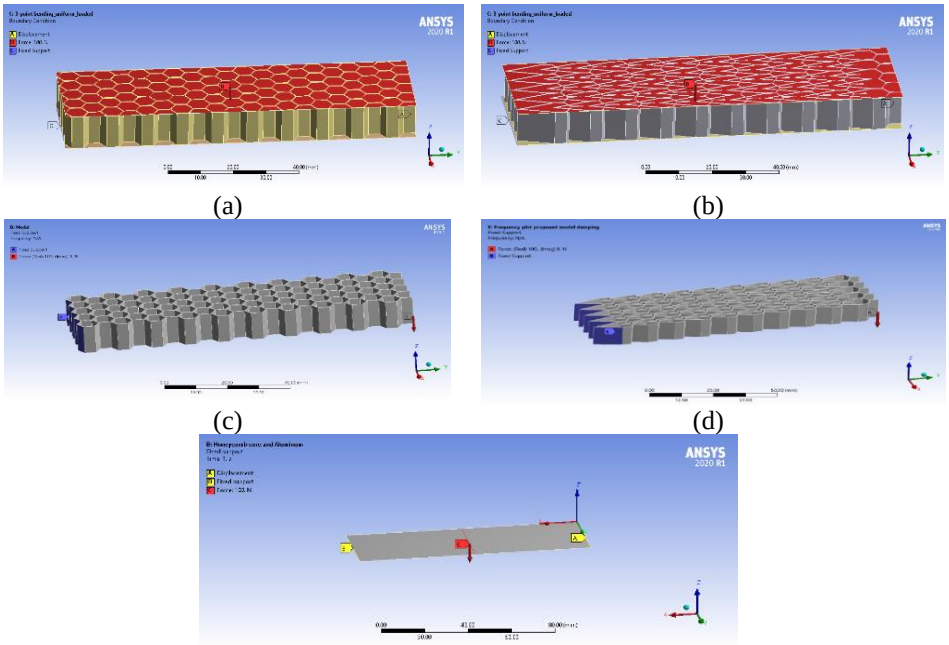

Fig. 3 Boundary conditions: (a) Loads and boundary condition of static analysis of normal hexagonal honeycomb sandwich beam; (b) Loads and boundary condition of static analysis of proposed honeycomb core sandwich beam; (c) Harmonic response boundary condition of honeycomb hexagonal core; (d) Harmonic response boundary condition of proposed honeycomb core; (e) 3-Point bending test of sandwich and boundary condition of equivalent shell model of honeycomb sandwich structure

3. Evaluation of Behavior of Sandwich Beam

In this section, approaches are identified to evaluate the stress in the core and skin of sandwich beams when they are subjected to flexural or shear loads.

3.1. Discrete sandwich modeling

The honeycomb sandwich beam is constructed with the complex hierarchical description of the core using a discrete modeling technique in the commercial software ANSYS. This method is made less preferable because it will take high computing time due to the cell details and a large number of cells involved in a full-scale honeycomb shell structure.

3.1.1. Equivalent sandwich model

In order to equate the bending rigidity of the honeycomb sandwich structure and the equivalent model, the honeycomb sandwich structure is now replaced by an equivalent model in ANSYS ACP, where all layers are identified and materials assigned.

3.2. Theoretical analysis

3.2.1. Sandwich beam

The sandwich beam is made up of two thin skins with a thickness of *t* and a core with a thickness of *c* as shown in Fig. 4. The overall depth of the beam is *h* and the width is *b*. The distance between the center lines of the upper and lower faces is *d*. *D* is the flexural stiffness of sandwich beam calculated by the following equation:

$$D = E_f \cdot \frac{bt^3}{6} + E_f \cdot \frac{btd^2}{2} + E_c \cdot \frac{bc^3}{12} \tag{1}$$

where E_f and E_c are elastic modulus of the face and core, respectively.

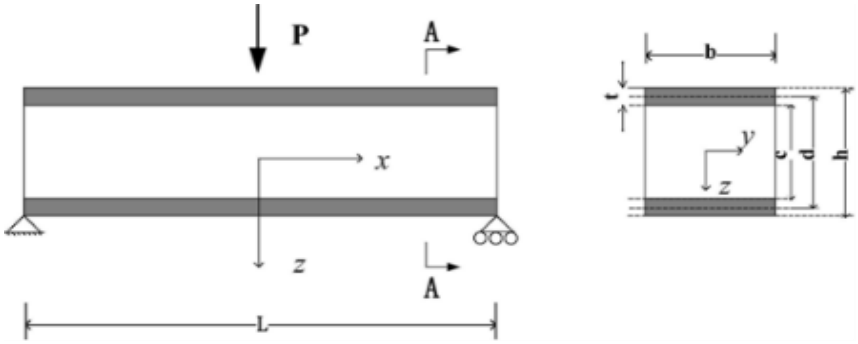

Fig. 4 Sandwich beam schematic model in three-point bending

The honeycomb core's elastic modulus is significantly lower than that of the face sheet. The face is only 0.5 mm thick, significantly thinner than the core, which measures 4 mm in height. The following equations are met:

$$3\left(\frac{d}{t}\right)^2 > 100{,}6\frac{E_f}{E_c}\frac{t}{c}\left(\frac{d}{c}\right)^2 > 100 \tag{2}$$

As a result, the first and third terms of Eq. (1) can be omitted [62]. Therefore, the total flexural stiffness supplied by the faces around the sandwich's centroid axis is determined as

$$D = E_f \cdot \frac{btd^2}{2} \tag{3}$$

When the sandwich beam is loaded by central point force *P*, according to the standard sandwich beam theory [62] , the usual stress on the face is at *x = L/2*,

$$\sigma_f = \frac{PLz}{4D} E_f \left(\frac{c}{2} \leqslant z \leqslant \frac{h}{2}, -\frac{h}{2} \leqslant z \leqslant -\frac{c}{2}\right) \tag{4}$$

The shear stress in the honeycomb core is

$$\tau_c = \frac{P}{2bd}\left(-\frac{c}{2} \leqslant z \leqslant \frac{c}{2}\right) \tag{5}$$

In the three-point bending, central deflection w of a sandwich beam is the sum of flexural deflection of the face sheets and shear deflection of the core.

$$w = T_1 + T_2 = -\frac{PL^3}{48D} - \frac{PL}{4AG_c} \tag{6}$$

where $A = bd^2/c$,G_c is the honeycomb core's shear modulus, and T_1 and T_2 are flexural and shear deflections at mid-span, respectively.

3.3. Analytical validation

In the literature, there are standard methods for calculating deflection and stresses. Ashby [63] introduced an equation of sandwich beams that can also be used to validate the aluminum sandwich and honeycomb core of the equivalent model of the finite element. Table 3 shows the validation and closeness between the simulation and analytical results of the sandwich flexural strength; hence, FEM can be used for validation. Analytical results were numerically obtained for the stress and strain of sandwich beam in the commercial ANSYS software shown in Tables 3 and 4. As a result of that, their characterization and prediction of most mechanical properties are known; similarly, this analysis was performed by Gibson [64].

Table 3 Comparison between simulation results and analytical calculated results

	Stress (N/mm)	Strain	Deformation (mm)
FEM	37.703	0.00053102	0.4297
Analytical	37.939	0.00053434	0.4254

3.4. FEM

The FEA is carried out in order to estimate the maximum stress and deflection under the three-point bending test of the sandwich beam. The values of the parameter used, face thickness t = 0.5 mm, core thickness c = 4mm, span L = 108 mm, beam width b = 35 mm, axial load in strut P = 100 N, moduli of elasticity of core E_c= 1 N/mm, moduli of elasticity of face sheet E_f = 71000 N/mm, the overall thickness of sandwich h = 5 mm, the distance between center-lines of opposite faces d = 4.5mm and shear modulus of honeycomb G_c = 70 N/mm. As shown in Table 3, the nearness of both results are in agreement, FEM still remains a valid method in analyzing and predicting the performance, strength and behavior of a component. A force of 100 N was used to keep the deformation of the sandwich beam in a linear state.

4. Results and Observation

4.1. Design of Experiments

4.1.1. Face sheet

An optimization was carried out to determine the best laminate angle ply orientation with the same thickness to reduce the total deformation of the sandwich based on the loading criteria considered. Three layer of the laminate each with two levels (0/90), a full factorial method is generated by the MATLAB code and imported to the ANSYS parameter set Workbench for evaluation while there is a 45% reduction in deformation when laminate layup ply angle is at (90,90,90,90,90) degree. This is in accordance with the fact that the UD carbon fiber has its highest strength at 90 degrees along its fiber axis. Moreover, this is due to the direction of load applied; therefore, (0, 90, 0, 90, 45, -45) degree is used; hence it gives reasonable stiffness irrespective of the direction of the applied load.

4.2. Static Analysis

4.2.1. Deformation and stresses

The sandwich beam is aligned in 3 point bending test setup, subjected to uniformly distributed load, and point load. Moreover, when a sandwich beam is loaded, internal forces develop within it to maintain equilibrium. In this case the internal forces have 3 components, compression, tension and shear force. Hence, the sandwich beam sagged and became shorter; therefore, the internal forces in the top became compressive, as a result, the bottom of the sandwich beam structure got longer and the normal forces in the bottom became tensile. The deformation and the stresses were observed as illustrated in Fig. 5. Fig. 5(a) shows that the sandwich beam is in compression on the top skin and tension on the bottom skin due to the applied load; the deflection occurs throughout the length of the sandwich beam, starting from the boundary conditions. The stresses keep increasing to the middle of the sandwich beam where the maximum bending stress and deformation occurred in the mid as shown in Fig. 5(b). It is observed that the maximum deflection occurred in the middle of the sandwich beam. Hence, Fig. 5(c) shows the rate of deformation of the sandwich beam along its length, starting gradually from both supports and reaching its maximum at the mid. Fig. 6 shows a stress plot along the top surface of the hexagonal honeycomb sandwich beam. Fig. 6(a) shows the geometry path of the hexagonal sandwich beam created along the top surface. It was investigated that the maximum stress equally occurred at the center of the honeycomb sandwich beam, the hollow nature of the hexagonal made the unstable nature of the line graph to be in a zig-zag manner as depicted in Fig. 6(b). It is as a result of errors; moreover, the force is either tension or compression along the line. Lastly, Fig. 7 depicts the stress plot along the top surface of the proposed honeycomb core model. Similarly, Fig. 7(a) shows the geometry path of the proposed sandwich created along the neutral axis while Fig. 7(a) depicts the stresses along the neutral axis. The simulation results plot is shown in Fig. 8. Where the hexagonal honeycomb was assigned 3 different materials and simulated in 3 point bending test, the same number of forces was applied and the stresses recorded for each amount of load. This was repeated for 3 materials, namely honeycomb, aluminum alloy and SAN foam. In Fig. 9 the same simulation setup was carried out but the hexagonal shaped core was replaced with the proposed core model. All the results were evaluated and plotted. It

was observed that there was significant stress resistance in the proposed model and it is also important to note that aluminum alloy became more elastic than the honeycomb material used in the hexagonal shaped core. To investigate the rate of deformation on sandwich structure for hexagonal shaped core, the materials were assigned and total deformation was recorded and plotted as shown in Fig. 10. The same was done for the proposed model in Fig. 11. It was observed that the proposed model has reasonable resistance to deformation irrespective of the material used. Finally, Fig. 12 shows the effect of core thickness to equivalent von Mises stress and shear stress. It was noted that when the core thickness is increased, both stresses decrease. The findings determined by means of the ANSYS workbench have been compared to the results calculated from the spreadsheet. The analysis of results reveals that the results of the FEM method and the analytical approach have less than 1% difference.

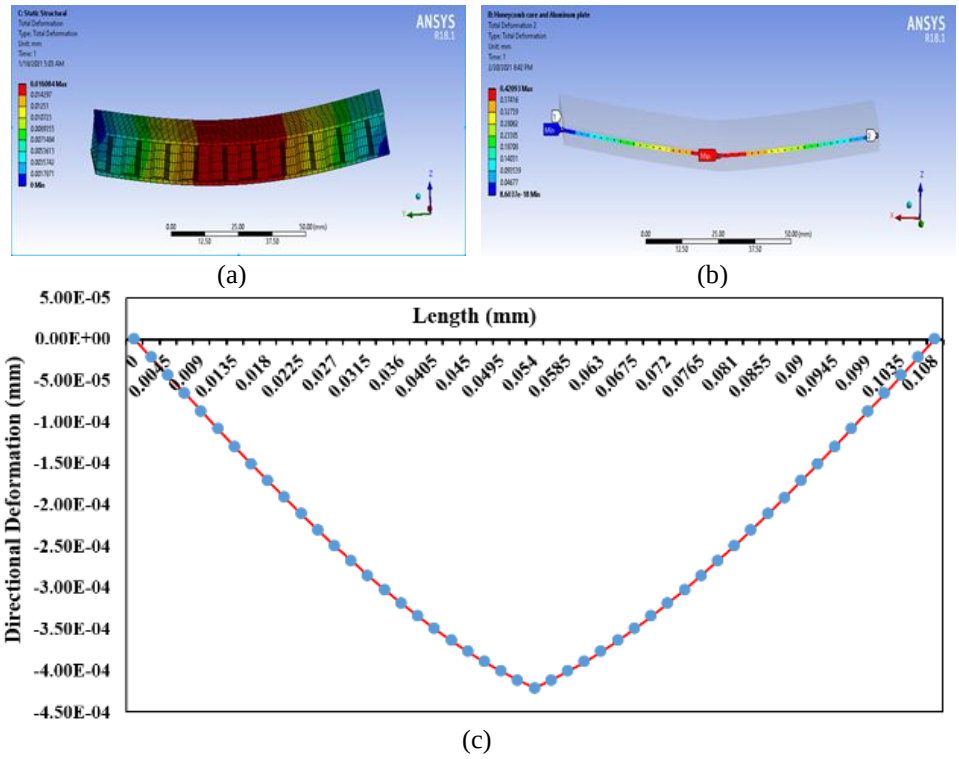

Fig. 5 Deflection along the surface of sandwich structure under 3-point bending loading (a) Total deformation of the sandwich beam; (b) Maximum deflection at the middle of the sandwich beam; (c) Directional deformation along the length of the sandwich beam

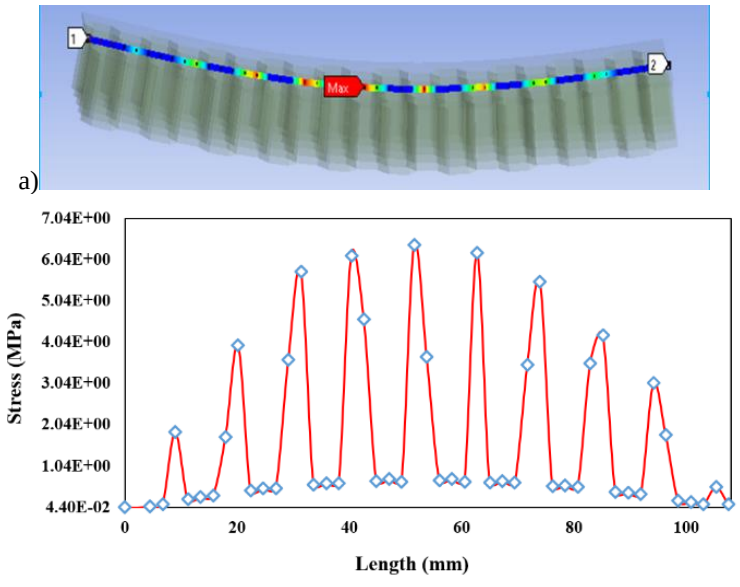

Fig. 6 Stress plot along the top surface of the hexagonal honeycomb structure (a) The geometry path on the top surface of the hexagonal honeycomb structure; (b) Stress plot along the length of the hexagonal honeycomb structure

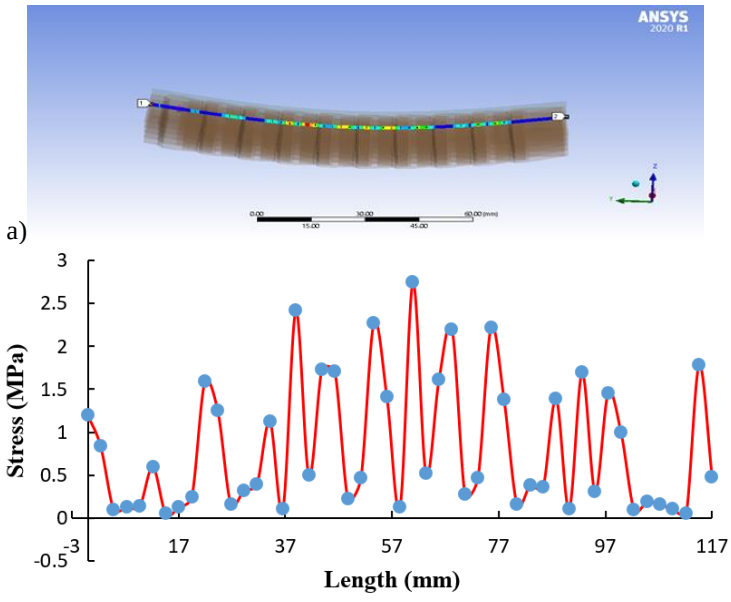

Fig. 7 Stress plot along the top surface of the proposed honeycomb structure (a) The geometry path on the top surface of the proposed honeycomb structure; (b) Stress plot along the length of the proposed honeycomb structure

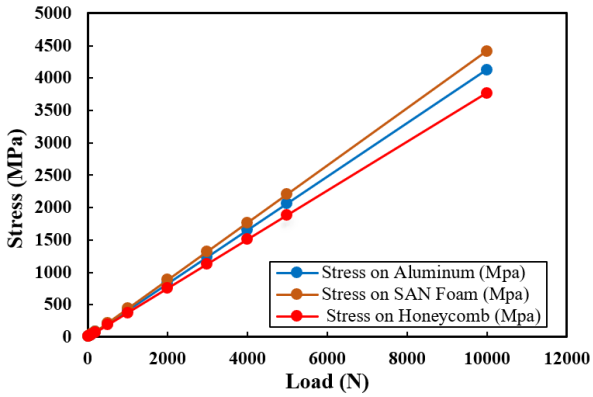

Fig. 8 Stresses comparison of hexagonal core materials to loading

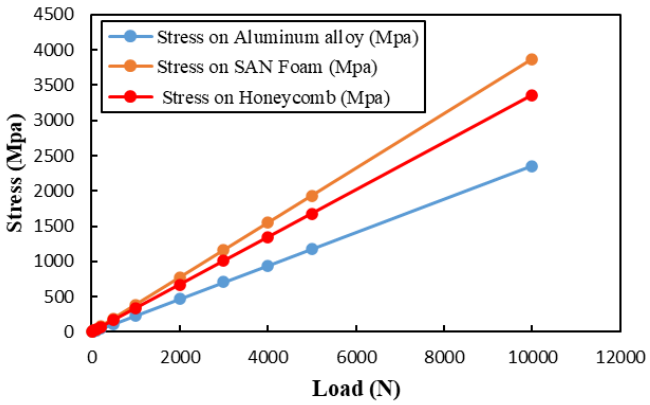

Fig. 9 Comparison of proposed core materials to loading

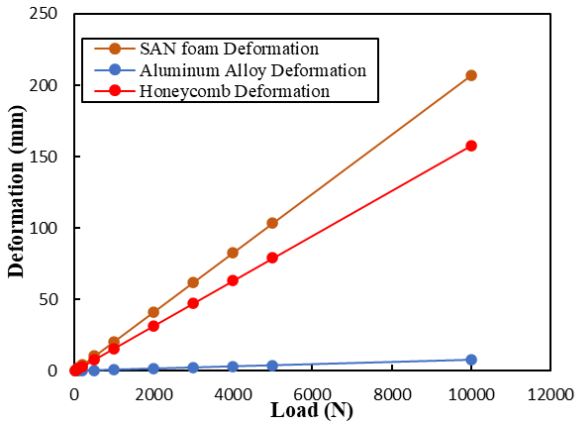

Fig. 10 Comparison of sandwich core deformation of hexagonal honeycomb core

Table 4 shows FEM and analytical results of the rate of change in length of the sandwich beam when load of 100 N is applied. The estimated stress of the sandwich beam can be obtained from the Eq. (7), combining the stress on the skin and the core. Table 5 depicts the comparison of stresses and validation analysis of the sandwich beam structure under 3-point bending test in analytical and FEM.

$$\sigma_s = \frac{M(h/2)}{(EI)_{eq}} E_s, \sigma_c = \frac{M(c/2)}{(EI)_{eq}} E_c \tag{7}$$

where h, c, $(EI)_{eq}$, E_c and E_s are sandwich height, core height, flexural stiffness, core young's modulus and skin young's modulus, respectively.

Table 4 Analytical and FEM results at force of 100 N compared

Method	Strain
FEM	0.00053102
Analytical	0.00053434

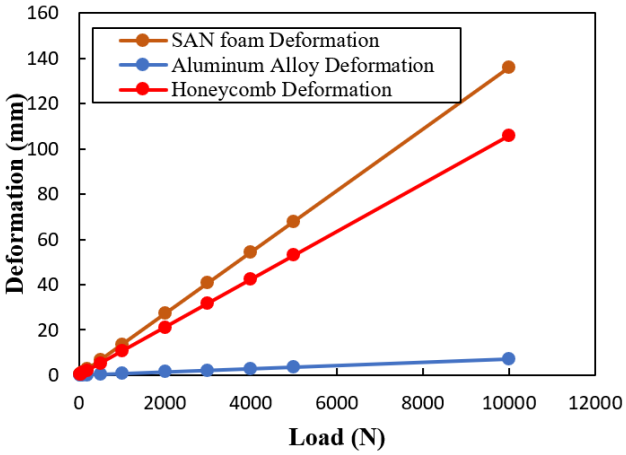

Fig. 11 Comparison of sandwich core deformation of proposed geometry core

Similarly, in order to investigate the proposed core model, the same parameter effect of applied load is maintained as used in hexagonal cores simulations. Hence, the behavior is similar to a hexagonal shaped model with improved stress resistance about 10.9%, 12.3%, 42.8% for honeycomb, SAN foam and aluminum alloy, respectively. In this case of the proposed shaped geometry simulation, aluminum became more elastic than honeycomb and foam materials compared to the hexagonal shaped core model. Response of the sandwich cores deformation in respect to the applied load. It is observed that aluminum core resists deformation more; it has very high compressive strength compared to foam honeycomb cores. This is similar to the work done by Aslan et al. [65]. He has found that the structure made of carbon fiber and aluminum honeycomb has the highest edgewise compression strength, but poor bending strength, and the structure made of polyurethane foam and carbon fiber has the greatest flat-wise compression strength and bending strength. Moreover, the deformation response of the proposed honeycomb model is similar to the

hexagonal honeycomb shaped core but deformation resistance improved by 32.9%, 12.9%, 34.4% for honeycomb, aluminum alloy and SAN foam core materials, respectively. Stress comparison of sandwich cores materials, aluminum, SAN foam and honeycomb of the same parameter effect of the applied load on the hexagonal shaped core. The stress is more on the foam core and lesser in honeycomb, irrespective of its lowest young's modulus and density. Hence, honeycomb is more elastic than aluminum and foam (Fig. 12). Effect of core thickness to shear stress and equivalent von Mises stress. Accordingly, as the core thickness increases both stresses decrease, this is in agreement with Potluri et al. [66] work.

Table 5 Equivalent Stress comparison of analytical and FEM

Force [N]	Equivalent Stress Analytical [MPa]	Equivalent Stress FEM [MPa]
10	3.77	3.79
20	7.54	7.59
30	11.31	11.38
40	15.08	15.18
50	18.85	18.97
60	22.62	22.76
70	26.39	26.56
80	30.16	30.35
90	33.93	34.14
100	37.70	37.94

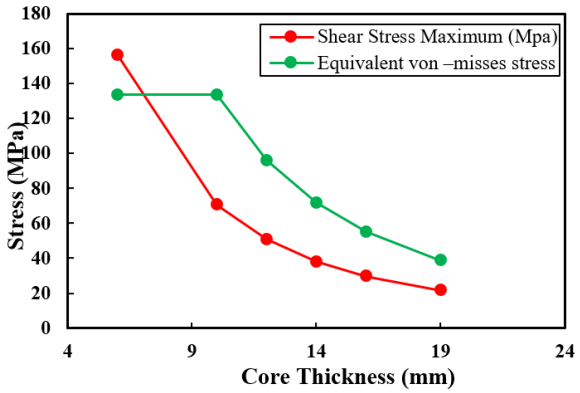

Fig. 12 Core thickness vs. stress

4.2.2. Proposed honeycomb core inclined edge model

The hexagonal honeycomb was modified in order to change its geometry to improve its strength and stiffness. Fig 1(d) is designed from the traditional hexagonal honeycomb structure and modified, with no addition in cell number, both having the same thickness and material. Hence, simulation was carried out in an ANSYS workbench with the same face sheet thickness and material properties; what changed was the core. It was discovered that the new shape has 79.9% deformation resistance; as a result, it is stiffer than a normal hexagonal structure. In general, for stiffer components honeycomb core inclined edge model should be used. Fig. 13 illustrates the strain resistance comparison between the

hexagonal core sandwich and the proposed core model of the sandwich beam. Hence, in order to investigate the extension of the hexagonal shaped core model and the proposed shaped core model in the ANSYS workbench mechanical, the sandwich beam was setup and assigned boundary condition in order to mimic the simply supported beam. The force ranging from 10 N to100 N was applied as a distributed load on the top surface of the sandwich structure and the corresponding strain recorded and plotted. The simulation was carried out with the same materials, parameters and loading; what changed was the shape of the core. It was observed that when the proposed core shape was used there was a significant reduction in the sandwich beam strain of the proposed shape core model.

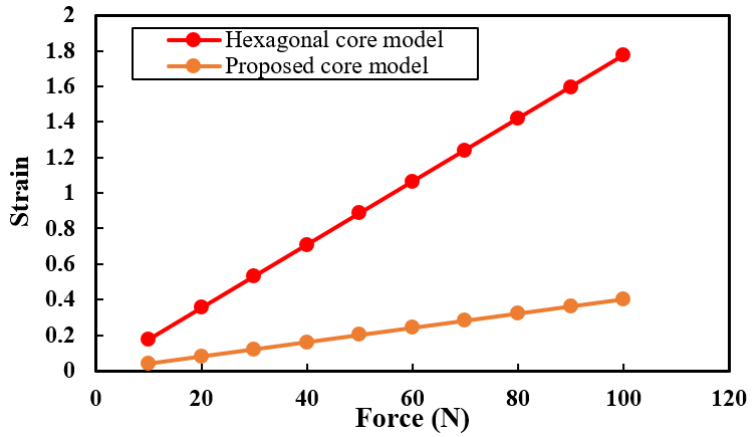

Fig. 13 Comparison between the hexagonal honeycomb sandwich beam and proposed shape core model sandwich beam

4.2.3. Analysis and comparison

Table 6 compares the results of the FEA and experimental data approaches done by Boudjemai [67] employed for the modal analysis of the hexagonal honeycomb sandwich beam under clamped-free boundary conditions. For comparison, the first three frequencies have been chosen and results recorded; hence a good agreement between the results is obtained. Furthermore, the proposed core sandwich structure was used with the same dimensions and materials as the experimental data provided by Boudjemai [67] in ANSYS and the results were compared as depicted in Table 6. Moreover, the first and third mode of the sandwich are in bending mode; the proposed core model shows great improvement in frequencies that will cause deformation on the sandwich beam, having 12.8% and 30.7% increase for the first and third mode, respectively.

Table 6 Comparison of Results

Frequency	FEA	Proposed model	Experimental[67]
1	133.45	151.75	134.5
2	309.69	308.21	311
3	818.51	929.69	711

4.3. Modal analysis and natural frequencies

Determination of the vibration characteristics assumes determination of natural frequency and mode shapes of the honeycomb sandwich structure. The natural frequency of the sandwich beam system comprises the frequencies at which it vibrates with increasing amplitude. Hence, the phenomenon is referred to as resonance. Fig. 14 shows the mode shapes of the first 6 natural frequencies on the sandwich beam structure with core thickness of 10mm and face thickness of 1mm. Fig. 15 depicts the mode shapes of natural frequency of honeycomb core and lastly Fig. 16 shows the first 6 modes shapes of natural frequency of proposed core. In addition, it has a significant effect on the shear stresses. This is due to the differences in mass and stiffness which is caused by variation in core and skin thickness of the honeycomb sandwich beam. Additionally this is in accordance with Upreti et al. [50] and Potluri et al. [66] work. Table 7 shows natural frequencies of the honeycomb sandwich beam structure, hexagonal honeycomb core and proposed core model.

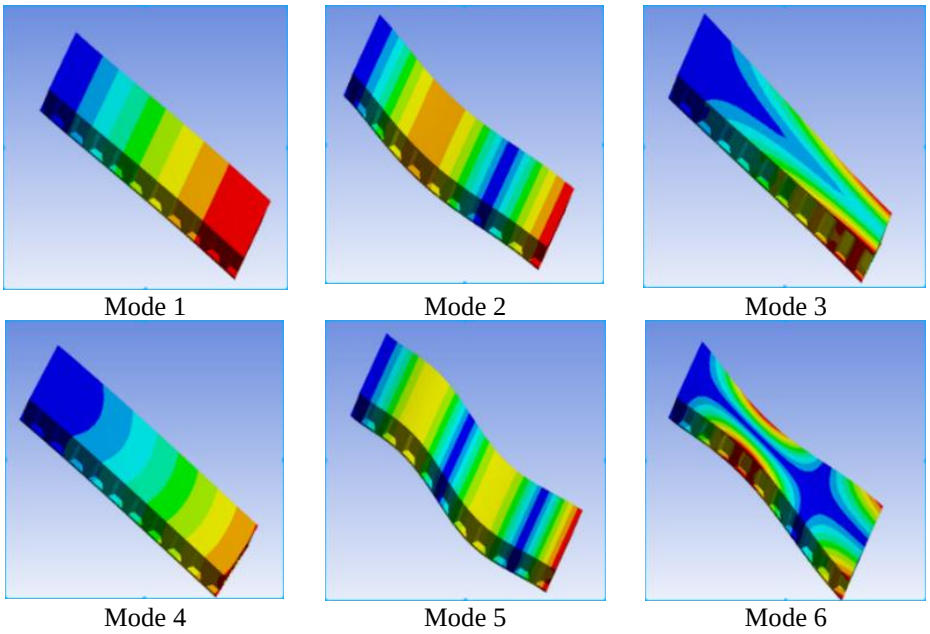

Fig. 14 First 6 mode shapes contours of the sandwich structure

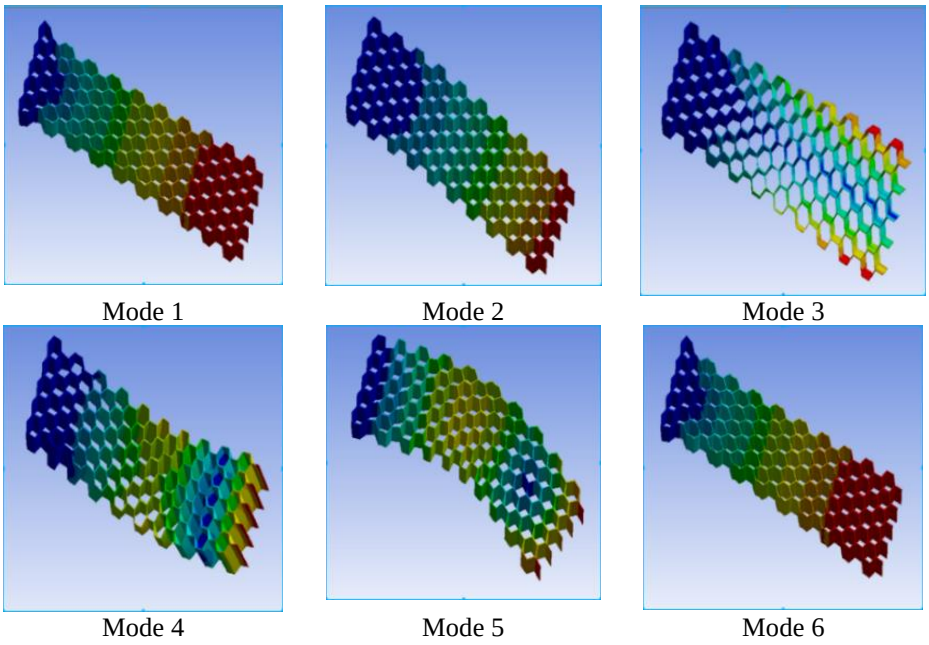

Fig. 15 First 6 mode shapes contours of honeycomb core

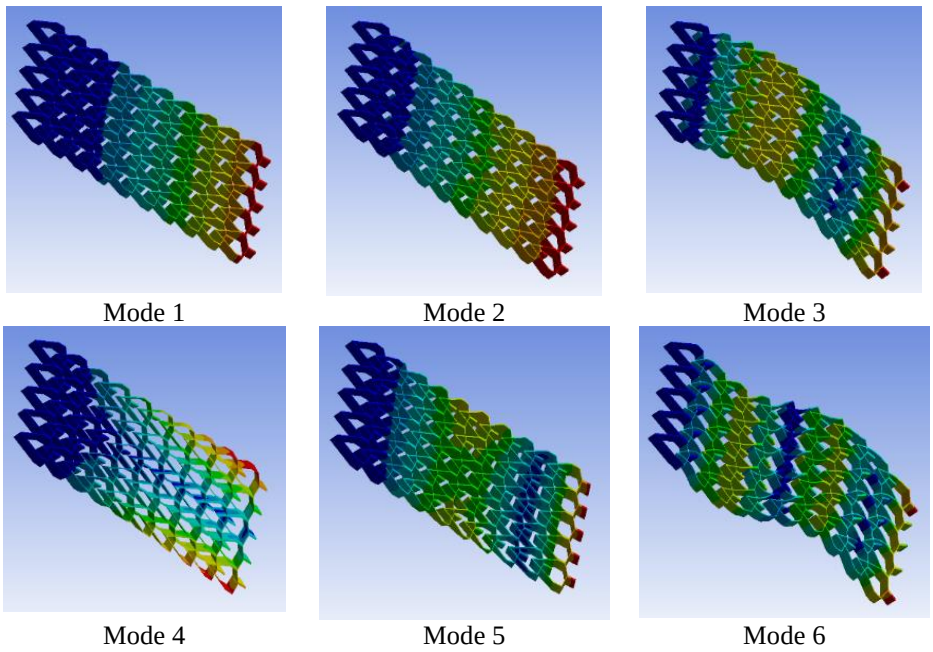

Fig. 16 First 6 mode shapes contours of proposed model

Table 7 Natural frequency

Mode	Natural frequency of sandwich beam (Hz)	Total deformation of sandwich beam (mm)	Natural frequency of honeycomb core model (Hz)	Total deform. of honeycomb core model (mm)	Natural frequency of proposed core model (Hz)	Total deformation of proposed core model (mm)
1	196.53	480.87	113.11	759.24	322.50	342.64
2	622.53	525.62	227.38	704.13	359.64	283.82
3	661.36	795.44	618.00	911.05	1242.30	317.00
4	990.69	680.32	702.54	819.35	1317.30	425.78
5	1148.40	583.92	1078.10	685.84	1868.20	382.03
6	1547.20	794.27	1327.30	507.74	2489.20	366.01

4.4. Honeycomb solid and equivalent model natural frequency

ACP in the ANSYS workbench was used to develop two types of honeycomb sandwich beam that give approximately the same results. A similar study was performed by Rahman et al. [68]. The models are shown in Fig.17. Fig. 17(a) shows the equivalent model designed from ACP where all the necessary material parameters are assigned. The solid model shown in Fig. 17(b) is also designed from the ACP and added solid layer; hence, using both is effective when considering the kind of boundary condition needed to apply. In addition, Table 8 depicts the difference in their nodes and elements and Table 9 shows the closeness of the equivalent model and solid model of sandwich beam mode results. The difference in their results is negligible; the equivalent model takes lesser time due to lower numbers of nodes and elements. A similar test was carried for the loading and deformation; it was found out that equivalent models run faster than the solid model. In addition, the solid model was added resin epoxy which made it stiffer than the equivalent model. In general, both models can be used for any analysis. This is in accord with Rahman et al. [68] study on the efficiency of continuum, discrete and equivalent models. The complex cellular geometry is converted into a set of effective continuum properties that can be employed in most sandwich calculations using these models.

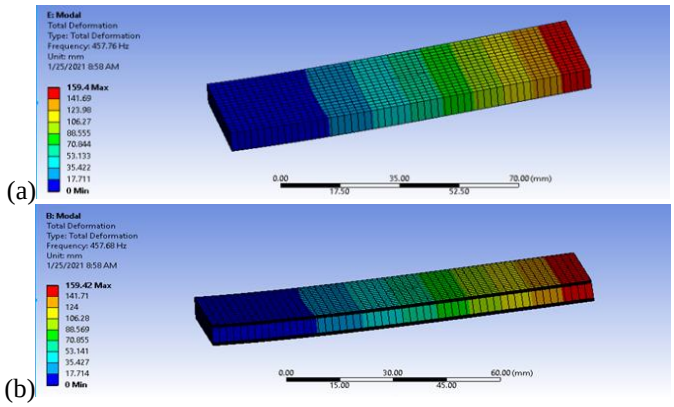

(a)

(b)

Fig. 17 Honeycomb sandwich beam structure (a) Equivalent model; (b) Solid model

Table 8 Nodes and elements of both models

Model	Nodes	Elements
Solid	11928	10153
Equivalent Shell	994	923

Table 9 Natural frequency comparison of results of equivalent model and solid model

Mode	Equivalent Frequency (Hz)	Solid Frequency (Hz)
1	457.76	457.68
2	2166.1	2181.5
3	2362	2364.3
4	2817	2819.2
5	6858.5	6915.8
6	7692.5	7710.8

4.4.1. Dynamic analysis and harmonic analysis

In order to effectively understand the significance of hexagonal honeycomb and the proposed honeycomb model designs, harmonic analysis is carried out. Additionally, the linear dynamics of forced frequency response analysis in the frequency domain of both models is observed.

4.4.2. Hexagonal honeycomb model

What is investigated is the behavior of the honeycomb structure under the steady-state sinusoidal (harmonic) loading at a given frequency. Moreover, the time-history response of the honeycomb will be ignored in this analysis. Therefore, what is taken into consideration is the honeycomb structure dynamic behavior in the frequency domain instead of the time domain. The two modes are spread over a frequency sweep from 0 to 900 Hz, modes while higher frequencies were ignored for this analysis. Hence, a single harmonic force of 100 N was applied in Z-axis orientation as shown in Fig 3(b). In order to obtain a reasonable resolution, the solution interval was made 50 and damping control ratio of 2%. Fig 18(a) depicts the frequency response plot of the honeycomb core, the peak frequencies were observed but for more accurate results in capturing the peak, a cluster was added for more resolution. In general, the frequency at which peak deformation occurs is 108 Hz, where the honeycomb core experiences the most deformation. However, with respect to this, contour results were created and evaluated Fig 18(b), while Fig 18(c) depicts the phase response plot. Lastly, considering the equivalent stresses, the model is set to the peak frequency of 108 Hz and the corresponding sweeping angle is the same as the directional deformation plot and was evaluated. Fig 18(d), in conclusion, based on the design criteria more material or FGM should be added in the region of a yellowish part to bring the stresses within a preferred reach in order to enable the honeycomb structure to overcome fatigue, and other harmful effects of forced vibration. The input and output of harmonic analysis are both sinusoidal acting at the same excitation frequency.

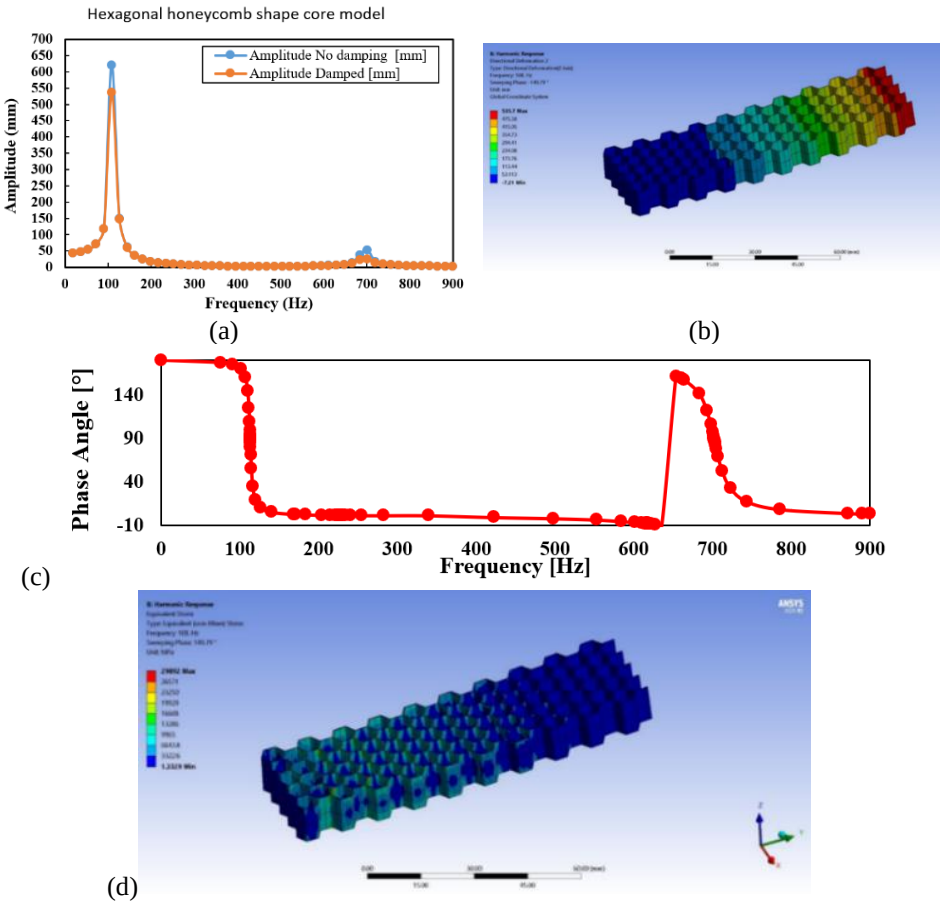

Fig. 18 Harmonic response of honeycomb core: (a) Frequency (Hz) vs. amplitude (mm) plot (maximum displacement in amplitude is dictated); (b) 108 Hz the maximum deformation occurred at the corresponding peak response and sweep angle 0f 149.79 °; (c) Phase response plot; (d) Equivalent stresses acting on the honeycomb core at the peak response

4.4.3. Proposed shape honeycomb core model

Similarly, the same steps were carried out as in hexagonal harmonic analysis for the proposed model. Fig. 19(a) shows the frequency response plot, Fig. 19(b) depicts the contour plot on the core, Fig. 20(a) illustrates the phase response plot of the proposed model and lastly, Fig. 20(b) shows the point of maximum bending. Hence, a damping ratio for the core is defined as 2%, under the harmonic system, a force of 100 N was applied in the Z direction, the one with the frequency sweep from 0 to 900 Hz. Moreover, the frequency at which peak deformation occurs is 324 Hz. The local results were recorded in Table 10.

However, as a result of that, the peak displacement occurs at the first natural frequency from the modal analysis of 324Hz while maximum spatial resolution is used. It is observed that the maximum value reported from the frequency response plot Fig 19(a) corresponds to the peak value on the contour plot as shown in Fig 19(b).

Table 10 Analysis and results

Model	Maximum frequency (Hz)	Phase angle (°)	Directional deformation (mm)	Equivalent stress (MPa)	Frequency sweep (Hz)	Harmonic force (N)
Hexagonal core	108	149.79	535.70	29892.00	0 - 900	100
Proposed core	324	93.614	69.76	21297.00	0 - 900	100

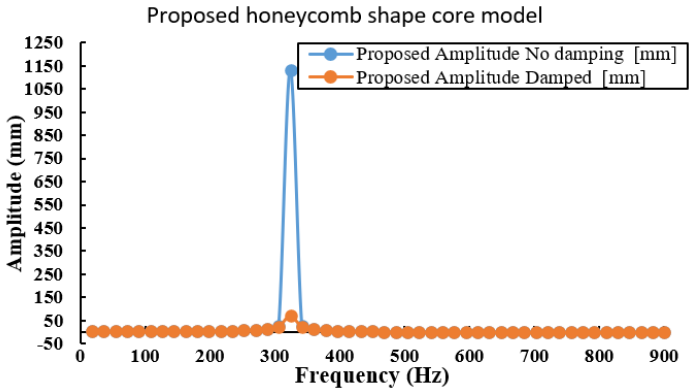

(a)

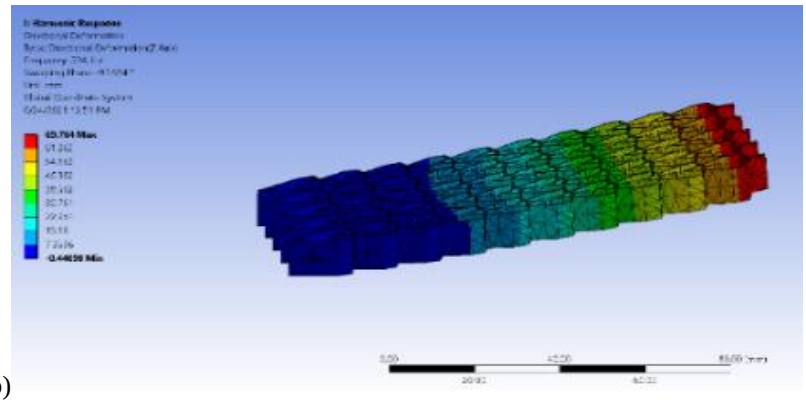

(b)

Fig. 19 Harmonic analysis of proposed honeycomb shape core: (a) Frequency response plot (maximum displacement in amplitude is dictated); (b) Directional deformation on the core at 324 Hz (contour plot)

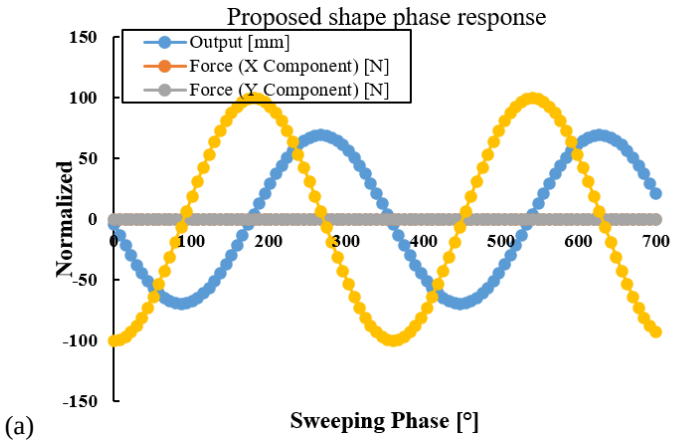

(a)

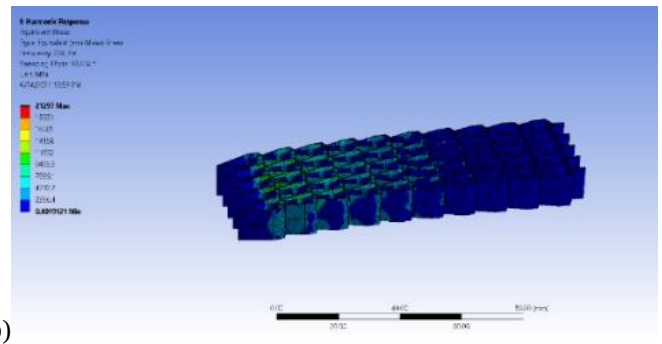

(b)

Fig. 20 Harmonic analysis of proposed honeycomb shape core: (a) 93.61° reflect a phase shift between the sinusoidal input loads and corresponding response due to 2% damping assumed in the proposed honeycomb model; (b) Equivalent stresses acting on the proposed honeycomb core at the peak response (point of maximum bending)

5. CONCLUSION

Both a comprehensive analysis and simulation were carried out and the results are depicted and plotted, and essential observation was noted. The stresses reviewed from the peak frequencies of both cores are analyzed. It is observed that the proposed core model has fewer stresses and deformation at a much higher frequency than the traditional hexagonal honeycomb core. It is clear that the distribution of mass and the stiffness in the proposed core model are better than the hexagonal shaped core as compared with the experimental results. The core thickness and the face sheet thickness have a significant effect on shear stress, deformation and equivalent maximum stress. Hence, increasing the thickness of the face sheets is the least efficient way to accomplish a rigid sandwich beam (not including the cost involved, especially when producing in large quantities) since it would increase the weight exponentially. Nevertheless, it was well observed that the type of core material affects its elastic behavior and strength of the sandwich beam. The skin thickness is directly proportional to mass and inversely proportional to the sandwich beam

structure's elastic strain. As a result of the simulation compared, the proposed shape core has 79.9% extension resistance more than the hexagonal shape core. Moreover, the equivalent sandwich beam model is the fastest to solve computationally, while the discrete sandwich beam model takes a longer time.

In general, we can conclude that sandwich beam structure with carbon fiber skin layers is stiffer than metal skins, lighter and of weight lesser. In addition, it was investigated that ply angle orientation has a significant effect on strength of the sandwich beam, same with the number of layers, but increasing the layers will equally increase the overall weight, instead the core thickness should be increased. In the situation of modal analysis, it was found that an increase in skin layers and core thickness increases the natural frequency; this is due to higher and lower stiffness in the modes. Therefore, the natural frequency was found to increase as core height increased. This is in line with a typical plate structure's vibration behavior. In the future, material selection for ductile failure and effect on loading in an uncontrolled environment of honeycomb sandwich beam structure should be clearly evaluated and the proposed shape of the core should have experimented with FGMs for more optimal results.

REFERENCES

1. Pandyaraj, V., Rajadurai, A., Anand, G., 2018, *Experimental investigation of compression strength in novel sandwich structure*, Materials Today: Proceedings, 5(2, Part 2), pp. 8625–8630.
2. Sorohan, Ş., Sandu, M., Sandu, A., Constantinescu, D.M., 2016, *Finite Element Models Used to Determine the Equivalent In-plane Properties of Honeycombs*, Materials Today: Proceedings, 3(4), pp. 1161–1166.
3. Ghongade, G., Kalyan, K.P., Vignesh, R.V., Govindaraju, M., 2021, *Design, fabrication, and analysis of cost effective steel honeycomb structures*, Materials Today: Proceedings, 46, pp. 4520–4526.
4. Qiu, C., Guan, Z., Guo, X., Li, Z., 2020, *Buckling of honeycomb structures under out-of-plane loads*, Journal of Sandwich Structures and Materials, 22(3), pp. 797–821.
5. Zhang, Z., Zhang, Q., Zhang, D., Li, Y., Jin, F., Fang, D., 2020, *Enhanced mechanical performance of brazed sandwich panels with high density square honeycomb-corrugation hybrid cores*, Thin-Walled Structures, 151, 106757.
6. Alshaer, A.W., Harland, D.J., 2021, *An investigation of the strength and stiffness of weight-saving sandwich beams with CFRP face sheets and seven 3D printed cores*, Composite Structures, 257, 113391.
7. Ashby, M.F., Gibson, L.J., 1997, *Cellular solids: structure and properties*, Press Syndicate of the University of Cambridge, Cambridge, UK, pp. 175–231.
8. Hussain, M., Khan, R., Abbas, N., 2019, *Experimental and computational studies on honeycomb sandwich structures under static and fatigue bending load*, Journal of King Saud University - Science, 31(2), pp. 222–229.
9. Burlayenko, V.N., Sadowski, T., 2009, *Analysis of structural performance of sandwich plates with foam-filled aluminum hexagonal honeycomb core*, Computational Materials Science, 45(3), pp. 658–662.
10. Rupani, S., Jani, S., Acharya, D., 2017, *Design, Modelling and Manufacturing aspects of Honeycomb Sandwich Structures: A Review*, International Journal of Science & Engineering Development Research, 2, pp. 526–532.
11. Li, Z., Yang, Q., Fang, R., Chen, W., Hao, H., 2021, *Crushing performances of Kirigami modified honeycomb structure in three axial directions*, Thin-Walled Structures, 160, 107365.
12. Kumar, A., Angra, S., Chanda, A.K., 2020, *Analysis of the effects of varying core thicknesses of Kevlar Honeycomb sandwich structures under different regimes of testing*, Materials Today: Proceedings, 21, pp. 1615–1623.
13. Alhijazi, M., Safaei, B., Zeeshan, Q., Asmael, M., 2021, *Modeling and simulation of the elastic properties of natural fiber-reinforced thermosets*, Polymer Composites, 42(7), pp. 3508–3517.
14. Zhang, Y., Li, Y., Guo, K., Zhu, L., 2021, *Dynamic mechanical behaviour and energy absorption of aluminium honeycomb sandwich panels under repeated impact loads*, Ocean Engineering, 219, 108344.
15. Zaid, N.Z.M., Rejab, M.R.M., Mohamed, N.A.N., 2016, *Sandwich structure based on corrugated-core: a review*, MATEC Web of Conferences, 74, 29.
16. Katariya, P. V, Panda, S.K., Mehar, K., 2021, *Theoretical modelling and experimental verification of modal responses of skewed laminated sandwich structure with epoxy-filled softcore*, Engineering Structures, 228, 111509.

17. Wang, Z., Tian, H., Lu, Z., Zhou, W., 2014, *High-speed axial impact of aluminum honeycomb - Experiments and simulations*, Composites Part B: Engineering, 56, pp. 1–8.
18. Liu, J., Tao, J., Li, F., Zhao, Z., 2020, *Flexural properties of a novel foam core sandwich structure reinforced by stiffeners*, Construction and Building Materials, 235, 117475.
19. Li, T., Wang, L., 2017, *Bending behavior of sandwich composite structures with tunable 3D-printed core materials*, Composite Structures, 175, pp. 46–57.
20. Wang, Y., Ermilov, V., Strigin, S., Safaei, B., 2021, *Multilevel modeling of the mechanical properties of graphene nanocomposites/polymer composites*, Microsystem Technologies, 27(12), pp. 4241–4251.
21. Chemami, A., Bey, K., Gilgert, J., Azari, Z., 2012, *Behaviour of composite sandwich foam-laminated glass/epoxy under solicitation static and fatigue*, Composites Part B: Engineering, 43(3), pp. 1178–1184.
22. Barbaros, I., Yang, Y., Safaei, B., Yang, Z., Qin, Z., Asmael, M., 2022, *State-of-the-art review of fabrication, application, and mechanical properties of functionally graded porous nanocomposite materials*, Nanotechnology Reviews, 11(1), pp. 321–371.
23. Li, X., Liu, W., Fang, H., Huo, R., Wu, P., 2019, *Flexural creep behavior and life prediction of GFRP-balsa sandwich beams*, Composite Structures, 224, 111009.
24. Ghanati, P., Safaei, B., 2019, *Elastic buckling analysis of polygonal thin sheets under compression*, Indian Journal of Physics, 93(1), pp. 47–52.
25. Ribeiro Faria, L.E., Gomes, G.F., de Sousa, S.R.G., Faria Bombard, A.J., Ancelotti Jr., A.C., 2020, *Dynamic experimental behavior of sandwich beams with honeycomb core filled with magnetic rheological gel: A statistical approach*, Smart Materials and Structures, 29(11), 115044
26. Katariya, P. V., Panda, S.K., 2019, *Numerical evaluation of transient deflection and frequency responses of sandwich shell structure using higher order theory and different mechanical loadings*, Engineering with Computers, 35(3), pp. 1009–1026.
27. Fazilati, J., Alisadeghi, M., 2016, *Multiobjective crashworthiness optimization of multi-layer honeycomb energy absorber panels under axial impact*, Thin-Walled Structures, 107, pp. 197–206.
28. Ha, G.X., Marinkovic, D., Zehn, M.W., 2019, *Parametric investigations of mechanical properties of nap-core sandwich composites*, Composites Part B: Engineering, 161, pp. 427–438.
29. Ha, G.X., Zehn, M.W., Marinkovic, D., Fragassa, C., 2019, *Dealing with Nap-Core Sandwich Composites: How to Predict the Effect of Symmetry*, Materials, 12(6), 874.
30. Lu, C., Zhao, M., Jie, L., Wang, J., Gao, Y., Cui, X., Chen, P., 2015, *Stress Distribution on Composite Honeycomb Sandwich Structure Suffered from Bending Load*, Procedia Engineering, 99, pp. 405–412.
31. Sakly, A., Laksimi, A., Kebir, H., Benmedakhen, S., 2016, *Experimental and modelling study of low velocity impacts on composite sandwich structures for railway applications*, Engineering Failure Analysis, 68, pp. 22–31.
32. Sahoo, B., Mehar, K., Sahoo, B., Sharma, N., Panda, S.K., 2021, *Thermal post-buckling analysis of graded sandwich curved structures under variable thermal loadings*, Engineering with Computers, doi:10.1007/s00366-021-01514-4
33. He, W., Liu, J., Tao, B., Xie, D., Liu, J., Zhang, M., 2016, *Experimental and numerical research on the low velocity impact behavior of hybrid corrugated core sandwich structures*, Composite Structures, 158, pp. 30–43.
34. Han, Q., Qin, H., Liu, Z., Han, Z., Zhang, J., Niu, S., Zhang, W., Sun, Y., Shi, S., 2020, *Experimental investigation on impact and bending properties of a novel dactyl-inspired sandwich honeycomb with carbon fiber*, Construction and Building Materials, 253, 119161.
35. Peng, C., Fox, K., Qian, M., Nguyen-Xuan, H., Tran, P., 2021, *3D printed sandwich beams with bioinspired cores: Mechanical performance and modelling*, Thin-Walled Structures, 161, 107471.
36. Harland, D., Alshaer, A.W., Brooks, H., 2019, *An Experimental and Numerical Investigation of a Novel 3D Printed Sandwich Material for Motorsport Applications*, Procedia Manufacturing, 36, pp. 11–18.
37. Sugiyama, K., Matsuzaki, R., Ueda, M., Todoroki, A., Hirano, Y., 2018, *3D printing of composite sandwich structures using continuous carbon fiber and fiber tension*, Composites Part A: Applied Science and Manufacturing, 113, pp. 114–121.
38. Liu, Y., Qin, Z., Chu, F., 2021, *Nonlinear forced vibrations of FGM sandwich cylindrical shells with porosities on an elastic substrate*, Nonlinear Dynamics, 104(2), pp. 1007–1021.
39. Li, H., Lv, H., Sun, H., Qin, Z., Xiong, J., Han, Q., Liu, J., Wang, X., 2021, *Nonlinear vibrations of fiber-reinforced composite cylindrical shells with bolt loosening boundary conditions*, Journal of Sound and Vibration, 496, 115935.
40. Liu, Y., Qin, Z., Chu, F., 2022, *Investigation of magneto-electro-thermo-mechanical loads on nonlinear forced vibrations of composite cylindrical shells*, Communications in Nonlinear Science and Numerical Simulation, 107, 106146.
41. Liu, Y., Qin, Z., Chu, F., 2021, *Nonlinear forced vibrations of functionally graded piezoelectric cylindrical shells under electric-thermo-mechanical loads*, International Journal of Mechanical Sciences, 201, 106474.
42. Yang, Y., Sahmani, S., Safaei, B., 2021, *Couple stress-based nonlinear primary resonant dynamics of FGM composite truncated conical microshells integrated with magnetostrictive layers*, Applied Mathematics and Mechanics (English Edition), 42(2), pp. 209–222.

43. Yang, Z., Lu, H., Sahmani, S., Safaei, B., 2021, *Isogeometric couple stress continuum-based linear and nonlinear flexural responses of functionally graded composite microplates with variable thickness*, Archives of Civil and Mechanical Engineering, 21(3), 114.
44. Sahmani, S., Safaei, B., 2021, *Microstructural-dependent nonlinear stability analysis of random checkerboard reinforced composite micropanels via moving Kriging meshfree approach*, European Physical Journal Plus, 136(8).pp. 1–31.
45. Liu, H., Safaei, B., Sahmani, S., 2021, *Combined axial and lateral stability behavior of random checkerboard reinforced cylindrical microshells via a couple stress-based moving Kriging meshfree model*, Archives of Civil and Mechanical Engineering, 22(1), pp. 1–20.
46. Moradi-Dastjerdi, R., Behdinan, K., 2021, *Temperature effect on free vibration response of a smart multifunctional sandwich plate*, Journal of Sandwich Structures and Materials, 23(6), pp. 2399–2421.
47. Moradi-Dastjerdi, R., Behdinan, K., 2021, *Free vibration response of smart sandwich plates with porous CNT-reinforced and piezoelectric layers*, Applied Mathematical Modelling, 96, pp. 66–79.
48. Katariya, P. V, Mehar, K., Panda, S.K., 2020, *Nonlinear dynamic responses of layered skew sandwich composite structure and experimental validation*, International Journal of Non-Linear Mechanics, 125, 103527.
49. Katariya, P. V., Panda, S.K., Mahapatra, T.R., 2019, *Prediction of nonlinear eigenfrequency of laminated curved sandwich structure using higher-order equivalent single-layer theory*, Journal of Sandwich Structures and Materials, 21(8), pp. 2846–2869.
50. Upreti, S., Singh, V.K., Kamal, S.K., Jain, A., Dixit, A., 2020, *Modelling and analysis of honeycomb sandwich structure using finite element method*, Materials Today: Proceedings, 25, pp. 620–625.
51. Gholami, M., Alibazi, A., Moradifard, R., Deylaghian, S., 2021, *Out-of-plane free vibration analysis of three-layer sandwich beams using dynamic stiffness matrix*, Alexandria Engineering Journal, 60(6), pp. 4981–4993.
52. Jin, Y., Jia, X.-Y., Wu, Q.-Q., Yu, G.-C., Zhang, X.-L., Chen, S., Wu, L.-Z., 2022, *Design of cylindrical honeycomb sandwich meta-structures for vibration suppression*, Mechanical Systems and Signal Processing, 163, 108075.
53. Safaei, B., 2021, *Frequency-dependent damped vibrations of multifunctional foam plates sandwiched and integrated by composite faces*, European Physical Journal Plus,doi:10.1140/epjp/s13360-021-01632-4
54. Kim, H.-Y., Hwang, W., 2002, *Effect of debonding on natural frequencies and frequency response functions of honeycomb sandwich beams*, Composite Structures, 55(1), pp. 51–62.
55. Abbadi, A., Tixier, C., Gilgert, J., Azari, Z., 2015, *Experimental study on the fatigue behaviour of honeycomb sandwich panels with artificial defects*, Composite Structures, 120, pp. 394–405.
56. Herranen, H., Pabut, O., Eerme, M., Majak, J., Pohlak, M., Kers, J., Saarna, M., Allikas, G., Aruniit, A., 2012, *Design and testing of sandwich structures with different core materials*, Medziagotyra, 18(1), pp. 45–50.
57. Alhijazi, M., Zeeshan, Q., Qin, Z., Safaei, B., Asmael, M., 2020, *Finite Element Analysis of Natural Fibers Composites: A Review*, Nanotechnology Reviews, 9(1), pp. 853–875.
58. Herranen, H., Pabut, O., Eerme, M., Majak, J., Pohlak, M., Kers, J., Saarna, M., Allikas, G., Aruniit, A., 2012, *Design and testing of sandwich structures with different core materials*, Medziagotyra, 18(1), pp. 45–50.
59. Selvaraj, R., Subramani, M., More, G., Ramamoorthy, M., 2021, *Dynamic responses of laminated composite sandwich beam with double-viscoelastic core layers*, Materials Today: Proceedings, 46, pp. 7468–7472.
60. Safaei, B., Fattahi, A.M., Chu, F., 2018, *Finite element study on elastic transition in platelet reinforced composites*, Microsystem Technologies, 24(6), pp. 2663–2671.
61. Pham, R.D., Hütter, G., 2021, *Influence of topology and porosity on size effects in stripes of cellular material with honeycomb structure under shear, tension and bending*, Mechanics of Materials, 154, 103727.
62. Allen, H.G., 1969, *Analysis and design of structural sandwich panels*, Pergamon Press, London, doi:10.1017/s0001924000051459
63. Ashby, M.F., Medalist, R.F.M., 1983, *Mechanical Properties of Cellular Solids*, Metall Mater Trans A, 14, pp. 1755–1769.
64. Ashby, M.F., Gibson, L.J., 1997, *Cellular solids: structure and properties*, Press Syndicate of the University of Cambridge, Cambridge, UK, pp. 175–231.
65. Aslan, M., Güler, O., Alver, Ü., 2018, *The Investigation of the Mechanical Properties of Sandwich Panel Composites with Different Surface and Core Materials*, Pamukkale University Journal of Engineering Sciences, 24(6), pp. 1062–1068.
66. Potluri, R., Eswara Kumar, A., Naga Raju, M., Babu, K.R.P., 2017, *Finite Element Analysis ofCellular Foam Core Sandwich Structures*, Materials Today: Proceedings, 4(2), pp. 2501–2510.
67. Boudjemai, A., Amri, R., Mankour, A., Salem, H., Bouanane, M.H., Boutchicha, D., 2012, *Modal analysis and testing of hexagonal honeycomb plates used for satellite structural design*, Materials and Design, 35, pp. 266–275.
68. Rahman, H., Jamshed, R., Hameed, H., Raza, S., 2011, *Finite element analysis (FEA) of honeycomb sandwich panel for continuum properties evaluation and core height influence on the dynamic behavior*, Advanced Materials Research, 326, pp. 1–10.